

Effect of laser intensity on the properties of carbon plasmas and deposited films

H. C. Ong and R. P. H. Chang

Department of Materials Science and Engineering, Northwestern University, 2225 North Campus Drive, Evanston, Illinois 60208

(Received 13 February 1996)

The effect of laser intensity on the deposition of diamondlike carbon (DLC) films has been studied using an ArF (193 nm) pulsed excimer laser. Our results are found to be distinct from other studies using Nd-YAG infrared or excimer 248-nm lasers. Two issues concerning the growth mechanism of the films are discussed: (1) the dynamics of the laser-induced plasma and (2) the dependence of the nature of the deposited films on laser intensity. To address the first issue, time-integrated optical emission spectroscopy has been carried out to investigate the carbon plasma induced by the ArF (193 nm) laser. Instead of molecular carbon bands (C_2), monoatomic neutral (C_I) and ionic (C_{II}) emission lines are found to dominate the spectra. The emissions of (C_I) and (C_{II}) have been studied as a function of laser intensity. For low laser intensity, the laser irradiation removes the target surface material primarily through thermal evaporation. When the laser intensity is above a threshold of $(3.7-4)\times 10^8$ W/cm², the evaporated species are also ionized. The observed phenomenon can be attributed to higher multiphoton ionization and inverse bremsstrahlung rate as the laser intensity is increased. For the second issue, films deposited at various intensities have been characterized by ellipsometry. Results show that films deposited at low intensity are found to have excellent optical transparency ($E_g=2.3$ eV), which implies a considerable amount of sp^3 bonds. However, films deposited at higher intensities are found to be more graphitic. The damage threshold has also been located at 3.7×10^8 W/cm². A qualitative structural analysis based on the effective-medium approximation has been performed on the deposited films to investigate the influence of laser intensity on their microstructures. [S0163-1829(97)01407-0]

INTRODUCTION

Pulsed laser deposition (PLD) has proven to be a viable technique for thin-film deposition.¹ Many thin-film materials such as high-temperature superconductors, semiconductors, and dielectric materials have been deposited by pulsed laser deposition.^{2,3} Among the materials, laser deposited diamondlike carbon (DLC) films have been demonstrated to possess some physical properties that are very close to crystalline diamond but distinct from chemical vapor deposition (CVD) hydrogenated amorphous carbon. DLC films are free of hydrogen, extremely hard, and consist of sp^3 C-C bond fractions higher than 70%.⁴⁻⁶ It is known that the degree of diamondlike character of the films is closely related to the deposition parameters such as substrate temperature, background pressure, as well as laser wavelength and intensity. Considerable studies have been made to improve the physical properties of DLC films, either by varying the laser power density⁵ or using an auxiliary energy source.⁷ Even though significant advances on DLC films have been achieved in recent years, understanding of the effect of laser-produced plasma on film properties is still lacking.⁸⁻¹² Laser plasma plume characterization is essential because it leads to an understanding of the interaction of various species within the plume, thereby opening the possibility of optimizing the properties of the films.

To date, much work on DLC films has been carried out using Nd-YAG (Ref. 5) or excimer 248 nm (Ref. 4) lasers; little is known of using an excimer laser at 193 nm. Recently, Xiong, *et al.* have deposited high-quality DLC films on silicon with C-C sp^3 bond fraction over 95% by ArF (193 nm) excimer laser.⁶ Compared with 248-nm KrF or longer-wavelength lasers used by other research groups, the laser

intensity Xiong *et al.* used was only 5×10^8 W/cm², which was at least one order of magnitude lower than those reported.⁶ The low laser intensity required to form high-quality films suggests that laser wavelength, in addition to intensity, may be important in controlling the physical and structural properties of DLC films. Hence, it is worthwhile to study the plasma plume produced by the ArF laser and compare to other available data obtained from longer wavelengths. In this study, time-integrated optical emission spectroscopy (TIOES) has been performed on investigating the composition of carbon plasma plume as a function of laser intensity as well as to elucidate the growth mechanism of DLC films. Results show that monoatomic carbon neutral and ion emission lines are found in our spectra. In addition, a transition at a laser intensity of $(3.7-4)\times 10^8$ W/cm² has been observed at which the carbon plasma is transformed from a laser thermal evaporation where neutral carbon is dominant to a laser plasma ionization where ionized carbon is dominant. The effect of the laser intensity on the quality of diamondlike carbon films is investigated. Films grown on Si(100) under various conditions are studied by spectroscopic ellipsometry. Results reveal that the structural and optical properties of the deposited films are strongly dependent on the laser intensity.

EXPERIMENTAL PROCEDURE

The schematic of the experimental setup has been described previously.¹⁴ Plasma characterization is carried out in a stainless steel ultrahigh vacuum chamber evacuated to a base pressure of 1×10^{-9} Torr using a turbomolecular pump and a cryopump. An ArF pulsed excimer laser (Questek Model 2740SC) with a wavelength of 193 nm and a pulse

width of 21 ns full width at half maximum (FWHM) is focused onto the surface of a 1-in. diameter pyrolytic graphite (PG) disk. The target is mounted at a 45° with respect to the laser beam and is constantly rotated to provide fresh surface for ablation. The energy of the laser is stabilized at 275 mJ/pulse and the repetition rate is kept at 5 Hz. The laser energy incident on the target is approximately 90% of the total energy due to losses from the focusing lens and the quartz window on the vacuum chamber. Various laser intensities are obtained by translating the focusing lens to change the irradiated beam size. The dimensions of the beam are determined using stylus profilometry to measure the area of craters. Time-integrated emission spectra are collected through a quartz window using an UV-grade optical fiber probe coupled to an Acton Research Corporation S-500 spectrometer with a 1200-groove/mm grating. A Princeton Applied Research 1455 silicon-based intensifier with high quantum efficiency is used to collect emission. This configuration allows a spectral resolution <0.5 nm and a wavelength range from 180 to 900 nm. The optical multichannel analyzer (Princeton Applied Research Model 1470 A) is used to process and store the emission spectra, and the background signal has been subtracted. The collection efficiency of the optical emission is enhanced by using a focusing lens with a focal length of 20 cm. The optical fiber probe is placed parallel to, and 1 to 3 mm away, from the target. The spectral response of the spectrometer-OMA system is calibrated using both a mercury and a neon lamp.

The silicon wafers used in this experiment are cleaned first in acetone and methanol, and then dipped into 1:1 HF/H₂O solution for 1 min. They are then transferred immediately into the vacuum chamber to avoid any contamination. Substrates are positioned parallel to and 60 mm away from the target. Deposition time ranges typically from 30 to 40 min yielding film thicknesses on the order of 300 to 500 Å. After deposition, a spectroscopic ellipsometer (SOPRA ES4G) in the rotating polarizer configuration is used to determine the optical properties of the films. The ellipsometric parameters, Tan Psi (Ψ) and Cos Delta (Δ), are measured for a range of wavelength (300 to 800 nm) at an incident angle of 75° with respect to the sample surface normal. A three-phase model with a structure of ambient/film/substrate is used to analyze the ellipsometric data.¹⁵ Surface and interface roughness are neglected in our model.^{6,16} This assumption can be justified by realizing that amorphous carbon films usually grow uniformly on smooth surfaces.¹⁷ Atomic force microscopy (AFM) has been carried out on our films for roughness measurements, and the results indicate that surface roughness is insignificant (less than 1 nm). Since measurements are carried out immediately after depositions, surface contamination is also ruled out from our model. The real (n) and imaginary (k) components of refractive indices and the thickness of the films are obtained by the best fit of our experimental curves with the Cauchy model given as¹⁵

$$n = A_1 + A_2/\lambda^2 + A_3/\lambda^4, \quad (1)$$

$$k = B_1 + B_2/\lambda + B_3/\lambda^3,$$

where λ is the photon wavelength, and A_i and B_i are the coefficients determined by the Marquardt least-squares routine to fit the experimental data. In fact, Xiong, Wang, and

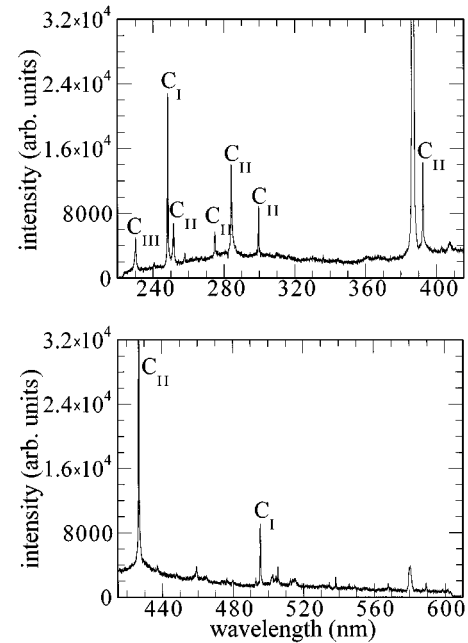


FIG. 1. Optical emission spectrum of carbon plasma taken from 220 to 620 nm at a laser intensity of 5×10^8 W/cm². C_I represents neutral carbon emission lines, C_{II} represents singly ionized carbon emission lines, and C_{III} represents doubly ionized carbon emission line.

Chang have shown previously the Cauchy model provides a good mathematical approximation to describe the dielectric functions of our diamondlike carbon films.¹⁶ The precision of the fits are double checked by measuring the thickness of the films using a stylus profilometer.

RESULTS

A. Plasma emission

The emission spectrum of laser-induced plasma obtained from a laser intensity of 5×10^8 W/cm² is shown in Fig. 1. Measurements are performed from 200 to 765 nm, but the spectrum is featureless beyond 600 nm. The spectrum consists of two broad continua with atomic carbon neutral and ionic emission lines superimposed on each other. Peaks located at 247.8, 437.2, 492.7, 505.3, and 538.1 nm are identified as neutral carbon (C_I) emissions,^{18,19} and a peak at 495.9 nm is the second order of 247.8 nm. Singly ionized carbon (C_{II}) emission peaks are located at 251.2, 257.62, 275.3, 284.4, 299.5, 392, 426.7, and 514.5 nm,^{18,19} and doubly ionized carbon (C_{III}) is located at 229.8 nm.^{18,19} Peaks at 386 and 580 nm are identified as laser lines. The presence of two continua can be attributed to (1) the free-free or free-bound electronic recombination of carbon species and electrons, and (2) the formation of larger molecules and cluster, both of which are common behaviors in the laser-induced plasma of graphite.²⁰

In contrast to the results reported by other research groups, no C₂ Swan band or C₂ high-pressure band are found in our spectra. Abhilasha *et al.*^{10,11} and Thareja and Abhilasha¹² used a Nd:YAG laser (1.06 μ m in 2.5 ns FWHM) to ablate graphite for optical emission measurement. At their lower-intensity power (1×10^{11} W/cm²) the

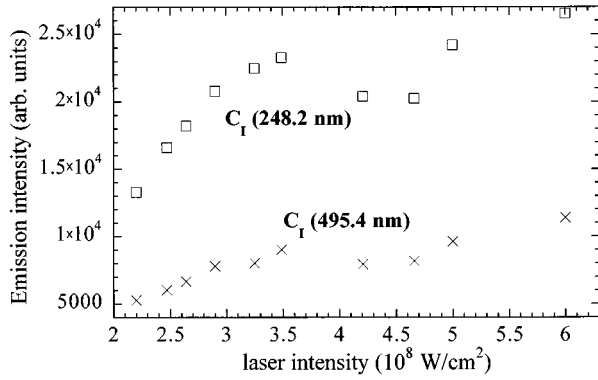


FIG. 2. Emission intensities of neutral carbon (C_I) at 248.2 nm (\square) and 495.4 nm (\times) vs laser intensity.

spectrum is dominated by C_2 emission bands. When the laser energy is increased to 4×10^{11} W/cm², C_2 Swan band, neutral and ionic atomic peaks from C_I to C_V are found to dominate equally. A KrF (248 nm) excimer laser at 7×10^8 W/cm² was used by Chen, Mazumder, and Purohit,⁸ but only a trace of atomic carbon emission superimposed on C_2 bands was observed. Recently, Muller *et al.*⁹ described the comparative study of laser deposition (KrF 248 nm) of amorphous carbon films using nanosecond and femtosecond pulse length. The intensity power used by them was 6.7×10^8 and 1.2×10^{13} W/cm², respectively. They found that the emission spectrum collected from femtosecond laser was dominated by C_{II} peaks rather than the C_2 Swan band that is usually given by nanosecond laser. Hence, it is suggested that there may exist a threshold value between 10^{10} and 10^{13} W/cm² for which C_I and C_{II} emissions are favorable.^{8,9} However, our spectrum shown in Fig. 1 is obtained with a laser intensity of 5×10^8 W/cm², which is considerably lower than the threshold value suggested by other researchers.

Emission spectra of various laser intensities ranging from 2.2×10^8 to 6×10^8 W/cm² are collected in an attempt to identify the threshold for C_2 emissions. The value of 2.2×10^8 W/cm² is chosen as our measurement limit because this value is believed to be one of the lowest laser powers for DLC film deposition.⁶ However, no C_2 bands are ever observed from our spectra. This observation makes us believe that not only the laser intensity but also the laser wavelength help to define the laser-induced plasma of carbon. Along with the results reported by Xiong *et al.*,⁶ we believe that the carbon atom and ion, instead of C_2 , play a major role in providing the properties of pulsed laser deposited amorphous carbon films that are close to those of diamond.

B. Laser intensity dependence

Even though our original idea is to locate the threshold value of C_2 emissions by varying the laser intensity, the results turn out to be very surprising. First of all, the color of the plasma plume changes abruptly from purple to pale blue as we reduce the laser intensity. This phenomenon indicates that there might exist a transition threshold in which the plasma undergoes some changes in its properties. The transition threshold is identified to be $\sim (3.5-4) \times 10^8$ W/cm². Dimensions of the plumes are also found to decrease with decreasing laser intensity.

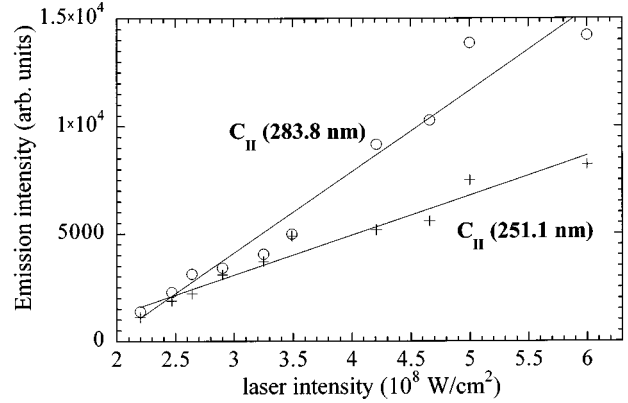


FIG. 3. Emission intensities of singly ionized carbon (C_{II}) at 283.8 nm (\circ) and 251.1 nm ($+$) vs laser intensity.

In order to study the nature of the laser-induced plasma, C_I at 247.8 and 495.4 nm and C_{II} at 251.1, 283.8, 392.3, and 426.3 nm emission lines at various laser intensities are examined in detail. The plot of emission intensities of C_I and C_{II} are shown in Figs. 2, 3, and 4. As we can see, the peak intensities of all carbon species increase as a function of laser intensity with C_I and C_{II} behave differently. Figure 2 shows that the emissions of C_I (248.2 and 495.4 nm) increase with increasing laser intensity, but suffer a slight depression when the intensity passes the transition threshold. For C_{II} emissions, however, two distinct behaviors were observed. The curves of C_{II} at 251.1 and 283.8 nm (Fig. 3) are found to increase steadily with increasing the laser intensity throughout the whole range. For C_{II} at 392.3 and 426.3 nm (Fig. 4), even though the emissions are found to increase very similarly to those in Fig. 3 from 2.2 to 3.8×10^8 W/cm², they experience a sharp rise after the threshold. Moreover, inspection of the slope of the curves implies that the emissions of C_I are more laser intensity dependent than that of C_{II} at intensity greater than threshold, but become less dependent at intensity less than threshold.

C. Optical properties

Figures 5(a) and 5(b) show the index of refraction (n) and extinction coefficient (k) spectra obtained by ellipsometry of diamondlike carbon films deposited on Si at laser

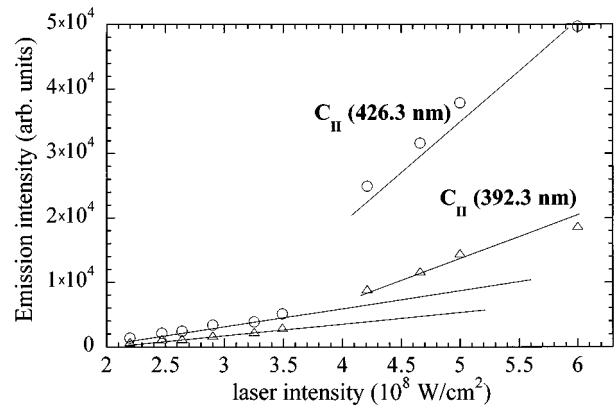


FIG. 4. Emission intensities of singly ionized carbon (C_{II}) at 426.3 nm (\circ) and 392.3 nm (\triangle) vs laser intensity.

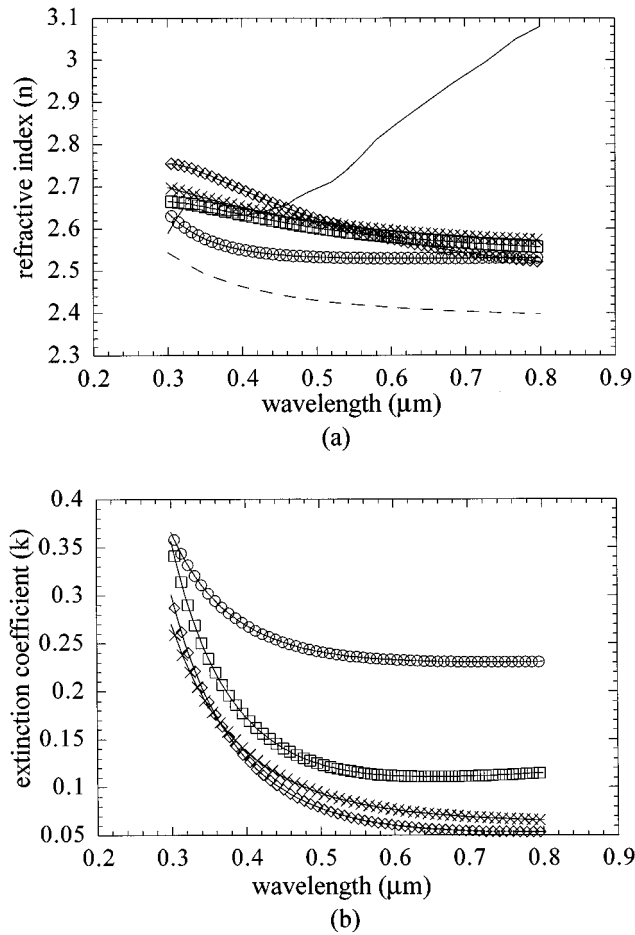


FIG. 5. (a), (b). The refractive index (n) and extinction coefficient (k) of DLC films deposited at various laser intensities as a function of wavelength. (\times) represents the laser intensity of $2.2 \times 10^8 \text{ W/cm}^2$; (\diamond) represents $3.7 \times 10^8 \text{ W/cm}^2$; (\square) represents $5 \times 10^8 \text{ W/cm}^2$; and (\circ) represents $6 \times 10^8 \text{ W/cm}^2$. The refractive indices of diamond and graphite are also shown as (-----) and (—), respectively.

intensities of 2.2×10^8 , 3.7×10^8 , 5×10^8 , and $6 \times 10^8 \text{ W/cm}^2$. The refractive indices (n) of natural diamond¹³ and graphite²¹ are also given for comparison. As we can see, the indices (n) of the films disperse with wavelength very similarly to crystalline diamond even though they all are slightly higher than that of diamond. Similar results have been reported by other research groups.⁴ The curve at $6 \times 10^8 \text{ W/cm}^2$ is the closest to diamond. As the extinction coefficients indicate, except the films deposited at low intensity ($2.2 \times 10^8 \text{ W/cm}^2$) and at threshold ($3.7 \times 10^8 \text{ W/cm}^2$), which show little difference, the films basically become more absorbing with increasing laser intensity. The thicknesses of the films predicted using ellipsometry have been confirmed by profilometry with good agreement.

Combining the n and k values with the corresponding photon energies E , the optical band gap E_g is calculated by using the relation $\epsilon(E) = B(E - E_g)^2/E^2$, where $\epsilon = 2nk$ and B is a constant.^{6,22} An example is presented in Fig. 6, in which the quantity $E\epsilon^{1/2}$ for a film deposited at $3.7 \times 10^8 \text{ W/cm}^2$ is plotted versus photon energy E . The x intercept provides the band gap and is found to be 2.3 eV. The optical

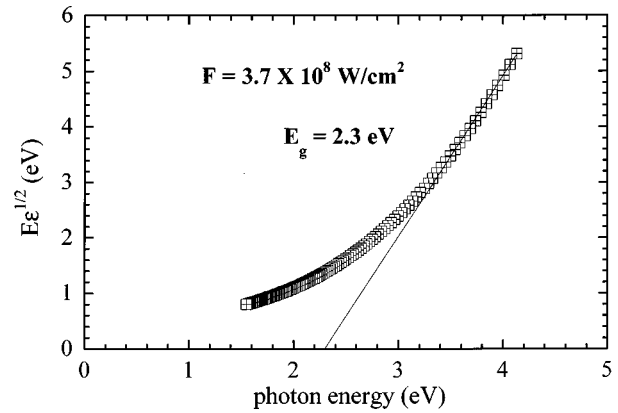


FIG. 6. Plot of $E\epsilon^{1/2}$ vs the photon energy E for film deposited at laser intensity of $3.7 \times 10^8 \text{ W/cm}^2$. The tangential extrapolation gives the optical band gap of the film of 2.3 eV.

gaps of other films determined by the same method are tabulated in Table I. As we can see, E_g increases from 2.2 to 2.3 eV when the laser intensity reaches the threshold and then falls to 1.5 eV at the intensity of $6 \times 10^8 \text{ W/cm}^2$.

D. Morphology

Figure 7 shows the atomic force microscopy (AFM) surface profiling of the carbon film on silicon deposited at $5 \times 10^8 \text{ W/cm}^2$. The surface is almost atomically smooth and featureless except with some small particulates deposited on top, which is very typical for pulsed laser deposition. All the other films show almost the same morphology and are relatively insensitive to the laser intensity. These findings support our argument on neglecting the surface roughness in our ellipsometric model.

DISCUSSION

When an excimer laser pulse with a duration of 20 ns and an intensity of the order of 10^8 W/cm^2 irradiates on the metal-like graphite surface, its leading edge is absorbed in the surface layer immediately with minor attenuation and transforms the material into a hot vapor.^{23–25} The interaction of the vaporized materials with part of the laser pulse results in the formation of an excited and ionized plasma adjacent to

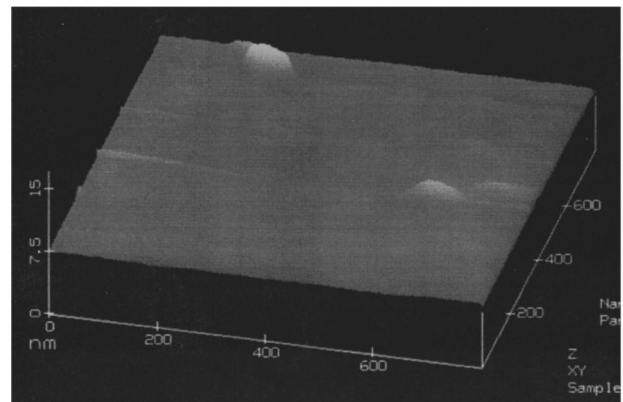


FIG. 7. The AFM surface profiling of DLC film on silicon at a laser intensity of $5 \times 10^8 \text{ W/cm}^2$.

TABLE I. The optical band gap (E_g) of amorphous carbon DLC films deposited at various laser intensity.

Laser intensity (10^8 W/cm 2)	E_g (eV)
2.2	2.2
3.7	2.3
5	2.1
6	1.5

the target. The degree of ionization of the plasma depends strongly on various parameters such as laser wavelength, laser intensity, and the intrinsic properties of ablated material. Basically, carbon ions can be generated from three mechanisms: (1) the multiabsorption of photons to the graphite surface and reach the ionization threshold of carbon (11.264 eV) [$C(s) + N h \nu \Rightarrow C^+(g) + e^-$], (2) the multiphoton ionization of gaseous carbon atoms to release ions [$C(g) + N h \nu \Rightarrow C^+(g) + e^-$] or the multiphoton absorption of atomic carbon to excited state and autoionized to ion, and (3) the collision of neutral atoms with energized electrons via inverse bremsstrahlung [$C(g) + e^- \Rightarrow C^+(g) + 2e^-$]. The third mechanism is, however, considered to be less important than the first two for the UV excimer laser due to the small absorption coefficient of electrons in the short-wavelength regime.^{23,26} The reactions are accompanied with substantial heating of the plasma by the laser and energy acquisition proceeds until the plasma becomes opaque to the irradiation. As the pulse is approaching its tail, the plasma attains sufficient energy and is allowed to expand freely in vacuum.

The observation of atomic carbon emissions rather than molecular emissions can be attributed to the high energy of photons bombarding the graphite surface. By realizing that the optical penetration depth decreases with decreasing wavelength, the efficiency of photon coupling to the surface of target is enhanced considerably by using 193-nm radiation.^{24,25} The surface layer, which corresponds to several monolayers, is heated up more intensively. The high surface temperature leads to an extensive bond breaking in the graphite and the vaporization of carbon atoms. Moreover, direct emissions of electrons and ions are made possible by this strong laser irradiation. As a result, a 193-nm radiation of 6.4 eV is sufficient to dissociate and release monoatomic carbon species but not the 5.5-eV photon energy of 248 nm or longer wavelength laser. The intensity threshold for C_2 emission in this experiment may be found to be as low as 10^7 W/cm 2 . This argument can be substantiated by our emission spectra collected at laser intensities down to 2.2×10^8 W/cm 2 , no C_2 emission bands are ever observed.

A simple model is given to understand the effect of laser intensity on the carbon plasma. Below the threshold, thermal evaporation is a dominant mechanism and direct ion and electron emission by the laser pulse is insignificant.²³ The plasma consists mostly of neutral carbon as evidenced by comparing the relative intensities of C_1 and C_{II} in Figs. 2, 3, and 4. The emission of C_1 increases with increasing the laser intensity due to the increase of laser sputtering rate on target. However, some ionization of carbon atoms may occur during their expansion in the Knudsen layer where the vapor atoms are strongly interacted with photons.²⁶ The density of free electron, at this point, is too low for inverse bremsstrahlung

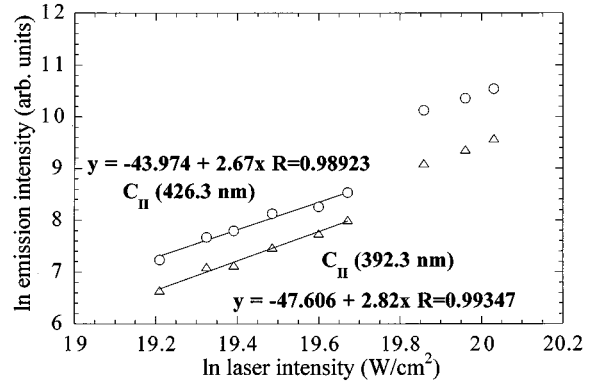


FIG. 8. The natural log-log plot of C_{II} emissions at 426.3 nm (\circ) and 392.3 nm (\triangle) vs laser intensity. The slope of the curves determined below threshold are 2.8 for 426.3 nm and 2.6 for 392.3 nm.

to have any effect on stripping the neutral. Thus, multiphoton ionization is considered to be the primary source for ion generation.²³ Assuming that the plasma is optically thin, which is valid for a weakly ionized plasma, the density of the carbon ion is roughly proportional to its emission intensity.²⁴ It is possible to estimate the number of photons needed to ionize a carbon atom by using the following equation based on Fermi's golden rule:^{27,28}

$$[C(II)] = A_n I^N, \quad (2)$$

where $[C(II)]$ is the relative emission intensity of C_{II} , A_n is a constant, I is the laser intensity, and N is the number of photons necessary to produce carbon ion. Figure 8 presents the natural log-log plots of emission intensity versus laser intensity for C_{II} at 392.3 and 426.3 nm. N values below threshold are determined to be 2.82 and 2.67 from the slopes of the plots and are also shown in Fig. 8. Result indicates that three photons are needed in order to generate a carbon ion and this bound-free transition is called "above-threshold ionization".²⁸ Experimental data for multiphoton ionization of atomic carbon are still lacking at this time to confirm our results, but theoretical calculations have been presented by Tang and Lambropoulos recently.²⁹ In their calculations, even though emphasis has been on the double ionization of atomic carbon and the energy photons Tang and Lambropoulos considered are higher than ours, they in fact point out that three photons are necessarily to be absorbed in order to ionize carbon atom.

When the laser intensity is increased above threshold, it heats up the plasma even more, leading to avalanche ionization of carbon atoms.²³ The high laser intensity creates a more effective coupling of photons to the carbon atoms than that of low intensity and subsequently produces more ions and free electrons. In addition, the increase of the number of free electron within the plasma enhances the absorption rate for inverse bremsstrahlung, which further generates more charged particles.^{23,30} This scenario, as observed in Figs. 4 and 8, actually happens at high laser intensity and causes an ascension of C_{II} emission and a shift of the y intercept in a log-log plot. Since the electron density in this regime is high enough to make the plasma become optically thick, emis-

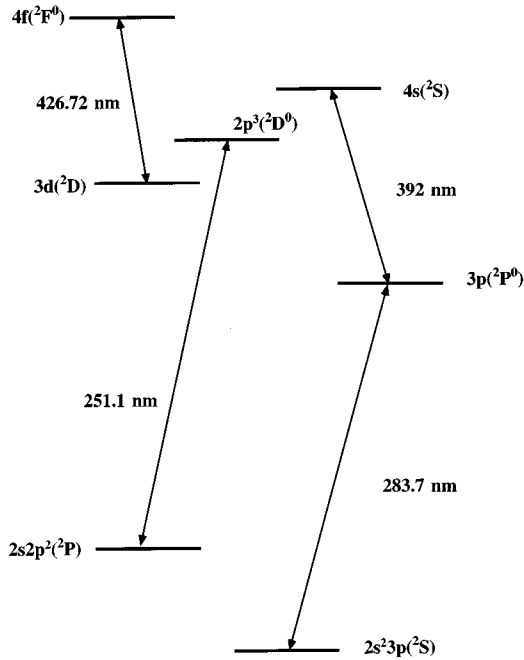


FIG. 9. The partial energy-level diagram of C_{II} .

sions are not able to escape from the plasma completely and collected by the OMA. Thus, the emission measurement results in an underestimation of the density of carbon ion and the slope determined here cannot provide any aspect of photon ionization. By examining the valley shown in Fig. 2 and the rise in Fig. 4, the trend of two curves reveals the production of ions at the expense of neutrals, which confirms our argument of assuming the ions are indeed produced within the plume but not from the target. The slight elevation of C_I emission afterward indicates that the sputtering rate on the target is faster than the ionization rate of carbon by multiphoton or inverse bremsstrahlung. The three-body recombination rate, which has an effect on reducing the ion density, is found to increase with laser intensity as indicated by the gradual evolution of the background emission continua²³ (not shown). However, the recombination is insignificant compared to ionization due to persistent increase of C_{II} emission even at very high intensity.²³ As we can see from the energy-level diagram of C_{II} (Ref. 18) shown in Fig. 9, the increase in the emissions at 392 and 426 nm reveal that the plume species actually acquire higher energies to reach higher excitation states and therefore undergo more excitations.

Films deposited at various laser intensities are found to have different optical properties. Basically, the diamondlike carbon films become more absorbing with increasing the laser intensity. It has been reported by Fallon *et al.* that a high-energy carbon ion may turn out to have an adverse effect on the carbon films.³¹ In their study, the energy of carbon ions was increased by further biasing the substrates and they found that the fraction of sp^3 actually decreased. Robertson^{32,33} has proposed that medium-energy ions bombard the surface and create a high compressive stress on the surface atomic layers which transform the local bonding of sp^2 to the metastable sp^3 configuration. Additional energy

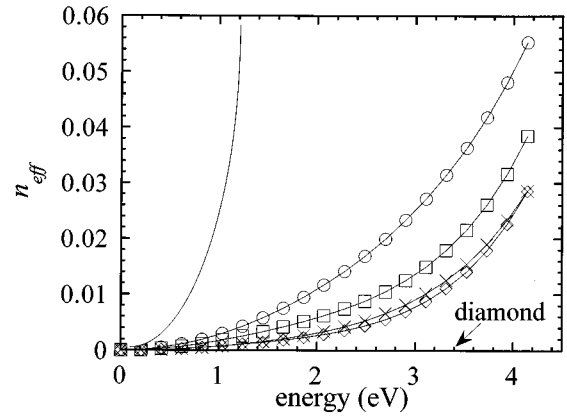


FIG. 10. The effective number n_{eff} of valence electrons per carbon atom vs photon energy. (\times) represents the laser intensity of $2.2 \times 10^8 \text{ W/cm}^2$, (\diamond) represents $3.7 \times 10^8 \text{ W/cm}^2$, (\square) represents $5 \times 10^8 \text{ W/cm}^2$, and (\circ) represents $6 \times 10^8 \text{ W/cm}^2$. Also shown are graphite (—) and diamond, respectively.

from ions will be largely released as heat and convert the metastable state back to the sp^2 stable state.

To investigate the structural change in DLC films with laser intensity, we examine the effective number of valence electrons per carbon atom taking part in the optical transition up to energy E_0 using the sum rule²²

$$n_{\text{eff}} = 7.66 \times 10^{-1} \frac{M}{\rho} \int_0^{E_0} E \epsilon_2(E) dE, \quad (3)$$

where M is the atomic weight of carbon, ρ is the density of the solid in kg^{-3} . For column IV materials, there are four valence electrons per atom available for bonding. If they all take part in interband optical transitions, we would expect n_{eff} approaching a value of 4 as all possible transitions are consumed at high photon energy.²² However, the situation is kind of different for carbon, which can exist in either tetrahedral or trigonal configurations. In graphite, since one electron per carbon atom is available for π bonding and is involved in the π - π^* transition, n_{eff} increases with photon energy to a value of 1 at about 9 eV.²² Above this energy the σ - σ^* transition begins and leads n_{eff} to approach to a value of 4 asymptotically. In diamond, on the other hand, n_{eff} would be kept at zero until the photon energy increases above 7 eV where the σ - σ^* transition begins to function.²² Hence, at low energy the behavior of n_{eff} could provide information on the local bondings of carbon in DLC films. Figure 10 illustrates the plots of n_{eff} versus energy for the corresponding DLC films. Since $\epsilon_2(E)$ spectra only cover the energy range from 1.5 to 4.5 eV, extrapolation to zero photon energy is performed in order to carry out the integrations. Plots of diamond and graphite are also given for comparison. Our results indicate the film deposited at $3.7 \times 10^8 \text{ W/cm}^2$ bares the most resemblance to diamond. Films behave more like graphite as laser intensity is increased further.

A structural analysis based on the effective-medium approximation (EMA) was performed on the films.³⁴ In general, it has been known that there are several limitations of using EMA to model diamondlike carbon.⁴ Hence, the results reported here are only to provide qualitative insight about the effect of high laser intensity on the microstructure

TABLE II. The fraction of sp^2 carbon in the DLC films determined by the effective-medium approximation.

Laser intensity (10^8 W/cm 2)	sp^2 (%)
2.2	3.6
3.7	3.4
5	5
6	14

of DLC films. A three phase model is defined where the film layer contains two different components, sp^3 and sp^2 carbon. The dielectric functions of each amorphous carbon component used in our model are extracted from Xiong *et al.*^{6,16} and Arakawa, Williams, and Inagaki.³⁵ The first has reported recently that the material is hydrogen free and contains sp^3 bond fraction over 95%, and the second material is deposited by thermal evaporation and is believed to consist of mostly sp^2 carbon. The results of the best fits are tabulated in Table II. It is shown that the percentage of sp^2 carbon is decreased from 3.6% to 3.4% when the laser intensity reaches the threshold and starts to increase to $\sim 14\%$ after the threshold. The amount of sp^2 determined here might be overestimated due to the uncertainty of the material's compositions obtained from Ref. 35. This finding is consistent to the results reported by Fallon *et al.*³ and we believe, as suggested by Roberston,^{32,33} the bombardment of high energy carbon ions helps relax the high-density sp^3 state to a low density graphitic phase. Voids, hydrogenated amorphous carbon, and crystalline diamond have been mixed with diamondlike carbon in an attempt to replace graphitic carbon, but this process did not work well. It indicates that amorphous sp^3 and sp^2 carbon are the only two compositions that give the best fit to our ellipsometric data.

CONCLUSIONS

Time-integrated optical emission spectroscopy has been carried out to investigate the carbon plasma induced by an ArF (193 nm) laser. In contrast to the results reported by other research groups, monoatomic carbon neutral and ion emission lines have been observed from our spectra. A transition of the plasma from a neutral dominated region to an ion dominated region is studied as a function of laser intensity. The value of the transition threshold is determined to be $\sim(3.5-4)\times 10^8$ W/cm 2 . The optical properties of the resulting films are found to be dependent upon the laser intensity, which in turn is related to the kinetic energy of ablated species. The most transparent film with a band gap of 2.3 eV is obtained at an intensity of 3.7×10^8 W/cm 2 where the transition threshold is roughly located. The effective-medium approximation revealed that the film deposited at the threshold indeed has the least amount of sp^2 graphitic carbon. Further analysis will be carried out to confirm our results. We believe, as reported by Fallon *et al.*,³¹ that a highly energetic carbon plasma might degrade the properties of the films instead of improving them. As a result, we have demonstrated that optical emission spectroscopy can provide an *in situ* nondestructive technique to optimize the growth process.

ACKNOWLEDGMENTS

The authors would like to thank F. Xiong for his technical assistance on system construction. This work was supported by Basic Energy Sciences Division of the U.S. Department of Energy. This research utilized MRL Central Facilities supported by the National Science Foundation at the Materials Research Center of Northwestern University.

- ¹J. T. Cheung and H. Sankur, *CRC Crit. Rev. Solid State Mater. Sci.* **15**, 63 (1988).
- ²H. Sankur, J. DeNatale, W. Gunning, and J. G. Nelson, *J. Vac. Sci. Technol. A* **5**, 2869 (1987).
- ³T. Venkatesan, X. D. Wu, A. Inam, Y. Jeon, M. Croft, E. W. Chase, C. C. Chang, J. B. Wachtman, R. W. Odom, F. R. diBrozolo, and C. A. Magee, *Appl. Phys. Lett.* **53**, 1431 (1988).
- ⁴D. L. Pappas, K. L. Saenger, J. Burley, W. Krakow, J. J. Cuomo, T. Gu, and R. W. Collins, *J. Appl. Phys.* **71**, 5675 (1992).
- ⁵C. B. Collins, F. Davanloo, E. M. Juengerman, W. R. Osborn, and D. R. Jander, *Appl. Phys. Lett.* **54**, 216 (1989).
- ⁶F. Xiong, Y. Y. Yang, V. Leppert, and R. P. H. Chang, *J. Mater. Res.* **8**, 2265 (1993).
- ⁷J. Krishnaswamy, A. Rengan, J. Narayan, K. Vedam, and C. J. McHargue, *Appl. Phys. Lett.* **54**, 2455 (1989).
- ⁸X. Chen, J. Mazumder, and A. Purohit, *Appl. Phys. A* **52**, 328 (1991).
- ⁹F. Muller, K. Mann, P. Simon, J. S. Bernstein, and G. J. Zaal, *SPIE Proc.* **1858**, 464 (1993).
- ¹⁰Abhilasha, P. S. R. Prasad, and R. K. Thareja, *Phys. Rev. E* **48**, 2929 (1993).
- ¹¹Abhilasha and R. K. Thareja, *Phys. Lett. A* **184**, 99 (1993).
- ¹²R. K. Thareja and Abhilasha, *J. Chem. Phys.* **100**, 4019 (1994).
- ¹³D. F. Edwards and H. R. Philipp, in *Handbook of Optical Constants of Solids*, edited by E. D. Palik (Academic, San Diego, 1985), p. 665.
- ¹⁴A. L. Yee, H. C. Ong, F. Xiong, and R. P. H. Chang, *J. Mater. Res.* (to be published).
- ¹⁵R. M. A. Azzam and N. M. Bashara, *Ellipsometry and Polarized Light* (North-Holland, Amsterdam, 1977).
- ¹⁶F. Xiong, Y. Y. Wang, and R. P. H. Chang, *Phys. Rev. B* **48**, 8016 (1993).
- ¹⁷R. W. Collins, *J. Vac. Sci. Technol. A* **7**, 1378 (1989).
- ¹⁸W. L. Wise, M. W. Smith, and B. M. Glennon, *Atomic Transition Probabilities, Vol. I, Hydrogen-Noen*, National Standard Reference Data System—NBS-4 (U.S. Government Printing Office, Washington, DC, 1966).
- ¹⁹R. C. Weast and M. J. Astle, *CRC Handbook of Chemistry and Physics*, 62nd ed. (CRC, Boca Raton, FL, 1982).
- ²⁰G. Koren and J. T. C. Yeh, *J. Appl. Phys.* **56**, 2120 (1984).
- ²¹A. Borghesi and G. Guizzetti, in *Handbook of Optical Constants of Solids II*, edited by E. D. Palik (Academic, San Diego, 1991), p. 449.

- ²²N. Savvides, *J. Appl. Phys.* **59**, 4133 (1986).
- ²³R. W. Dreyfus, *J. Appl. Phys.* **69**, 1721 (1991).
- ²⁴Y. W. Kim, in *Laser Induced Plasma and Applications*, edited by L. J. Radziemski and D. A. Cremers (Marcel Dekker, New York, 1991), p. 327.
- ²⁵R. K. Singh and J. Narayan, *Phys. Rev. B* **41**, 8843 (1990).
- ²⁶R. Kelly and R. W. Dreyfus, *Surf. Sci.* **198**, 263 (1988).
- ²⁷J. J. Gaumet, A. Wakisaka, Y. Shimizu, and Y. Tamori, *J. Chem. Soc. Faraday Trans.* **89**, 1667 (1993).
- ²⁸P. Agostini and G. Petite, *Contemp. Phys.* **29**, 57 (1988).
- ²⁹X. Tang and P. Lambropoulos, *Phys. Rev. Lett.* **58**, 108 (1987).
- ³⁰J. T. Ready, *Effects of High Power Laser Radiation* (Academic, New York, 1971).
- ³¹P. J. Fallon, V. S. Veerasamy, C. A. Davis, J. Robertson, G. A. J. Amaratunga, W. I. Milne, and J. Koskinen, *Phys. Rev. B* **48**, 4777 (1993).
- ³²J. Robertson, *Philos. Trans. R. Soc. London A* **342**, 227 (1993).
- ³³J. Robertson, *Diamond Relat. Mater.* **2**, 984 (1993).
- ³⁴D. E. Aspnes, in *Handbook of Optical Constants of Solids*, edited by E. D. Palik (Academic, San Diego, 1985), p. 89.
- ³⁵E. T. Arakawa, M. W. Williams, and T. Inagaki, *J. Appl. Phys.* **48**, 3176 (1977).